AMERICAN SOCIETY FOR MICROBIOLOGY | Applied and Environmental Microbiology®

GENETICS AND MOLECULAR BIOLOGY

The Autophagy Gene *BcATG8* Regulates the Vegetative Differentiation and Pathogenicity of *Botrytis cinerea*

Weichao Ren,[a] Na Liu,[b] Chengwei Sang,[a] Dongya Shi,[a] Mingguo Zhou,[a] Changjun Chen,[a] Qingming Qin,[c] Wenchan Chen[a]

[a]College of Plant Protection, Nanjing Agricultural University, Nanjing, Jiangsu, China
[b]Institute of Biotechnology, Zhejiang University, Hangzhou, Zhejiang, China
[c]College of Plant Sciences, Jilin University, Changchun, Jilin, China

ABSTRACT Autophagy is a conserved degradation process that maintains intracellular homeostasis to ensure normal cell differentiation and development in eukaryotes. *ATG8* is one of the key molecular components of the autophagy pathway. In this study, we identified and characterized *BcATG8*, a homologue of *Saccharomyces cerevisiae* (yeast) *ATG8* in the necrotrophic plant pathogen *Botrytis cinerea*. Yeast complementation experiments demonstrated that *BcATG8* can functionally complement the defects of the yeast *ATG8* null mutant. Direct physical interaction between BcAtg8 and BcAtg4 was detected in the yeast two-hybrid system. Subcellular localization assays showed that green fluorescent protein-tagged BcAtg8 (GFP-BcAtg8) localized in the cytoplasm as preautophagosomal structures (PAS) under general conditions but mainly accumulated in the lumen of vacuoles in the case of autophagy induction. Deletion of *BcATG8* (Δ*BcAtg8* mutant) blocked autophagy and significantly impaired mycelial growth, conidiation, sclerotial formation, and virulence. In addition, the conidia of the Δ*BcAtg8* mutant contained fewer lipid droplets (LDs), and quantitative real-time PCR (qRT-PCR) assays revealed that the basal expression levels of the LD metabolism-related genes in the mutant were significantly different from those in the wild-type (WT) strain. All of these phenotypic defects were restored by gene complementation. These results indicate that *BcATG8* is essential for autophagy to regulate fungal development, pathogenesis, and lipid metabolism in *B. cinerea*.

IMPORTANCE The gray mold fungus *Botrytis cinerea* is an economically important plant pathogen with a broad host range. Although there are fungicides for its control, many classes of fungicides have failed due to its genetic plasticity. Exploring the fundamental biology of *B. cinerea* can provide the theoretical basis for sustainable and long-term disease management. Autophagy is an intracellular process for degradation and recycling of cytosolic materials in eukaryotes and is now known to be vital for fungal life. Here, we report studies of the biological role of the autophagy gene *BcATG8* in *B. cinerea*. The results suggest that autophagy plays a crucial role in vegetative differentiation and virulence of *B. cinerea*.

KEYWORDS *BcATG8*, *Botrytis cinerea*, autophagy, vegetative differentiation, virulence

Botrytis cinerea, a model plant-pathogenic fungus that causes gray mold and rot disease in a wide range of crop species, has been considered the second most important phytopathogen on the basis of its economic and scientific implications (1). Since cultivars with effective resistance to *B. cinerea* are limited, chemical control still plays a pivotal role in an integrated control program (2). However, *B. cinerea* is difficult to control owing to its numerous attack modes, genetic versatility, and diverse host inoculum sources, and even worse, it can survive as mycelia and conidia or for extended periods as sclerotium in crop debris under adverse conditions (3). The serious damage caused by control failure highlights the need for the development of feasible disease

Received 6 November 2017 **Accepted** 28 February 2018

Accepted manuscript posted online 23 March 2018

Citation Ren W, Liu N, Sang C, Shi D, Zhou M, Chen C, Qin Q, Chen W. 2018. The autophagy gene *BcATG8* regulates the vegetative differentiation and pathogenicity of *Botrytis cinerea*. Appl Environ Microbiol 84:e02455-17. https://doi.org/10.1128/AEM.02455-17.

Editor Janet L. Schottel, University of Minnesota

Address correspondence to Changjun Chen, changjun-chen@njau.edu.cn, or Qingming Qin, qmqin@jlu.edu.cn.

control strategies, which may be derived from the understanding of fungal biology and the mechanisms of host-pathogen interaction.

Macroautophagy (here called autophagy) is a tightly controlled cellular degradation process that guarantees the quality and quantity of cytoplasmic components through their sequestration within double-membrane autophagosomes that are delivered to vacuoles/lysosomes for digestion (4, 5). Consequently, the indispensable recycled materials can be reprocessed not only for the synthesis of new macromolecules but also as a cellular energy source, which attributes an imperative role to autophagy in response to nutrient starvation or under specific physiological conditions requiring extensive cellular remodeling, such as cell differentiation and development (6, 7).

To date, a variety of autophagy-related (ATG) genes have been identified and functionally characterized (8). In the *Saccharomyces cerevisiae* (yeast) model, 36 ATG genes have been well studied, which has led to a preliminary understanding about the mechanism and function of autophagy (9, 10). Of these, *ATG8* is a key molecular element of the autophagy pathway, first found in *S. cerevisiae*, that plays a major role in the formation of autophagosomes (11). The *ATG8*-encoded protein, Atg8, is a membrane-bound ubiquitin-like protein that associates with the autophagosome membrane and microtubule and is used extensively as a autophagy marker (12), since the amount of Atg8-phosphatidylethanolamine (PE) correlates well with the extent of autophagosome formation (13, 14).

Gene function studies have indicated the involvement of *ATG8* in various physiological processes, such as fungal development, pathogenesis, and secondary metabolism, in filamentous fungi (15, 16). In *Podospora anserina*, deletion of the *ATG8* gene (*PaATG8*) resulted in fewer aerial hyphae, no pigmentation, and protoperithecia (17). Deletion of the *ATG8* gene in *Aspergillus oryzae* (*AoATG8*) impairs its production of aerial hyphae and conidial germination (18). In *Magnaporthe oryzae*, the *ATG8* gene (*MoATG8*) mediates autophagic cell death and is required for the formation of the infection structure (19, 20). In *Fusarium graminearum*, mutants lacking the *ATG8* gene (*FgATG8*) show defects in aerial hyphal growth, reproductive development, and mycotoxin biosynthesis (21). In the insect pathogen *Metarhizium robertsii*, the *ATG8* gene (*MrATG8*) is required for fungal development, lipid storage, and virulence (22). Despite the knowledge about the roles of *ATG8* in various filamentous fungi, its role in *B. cinerea* remains obscure. In the present study, we characterize the autophagy gene of *B. cinerea*, *BcATG8*, and describe its involvement in vegetative differentiation and virulence.

RESULTS

Identification of *BcATG8* in *B. cinerea*. Twenty-two autophagy-related genes have been identified by homologous alignment in the *B. cinerea* genome (see Table S1 in the supplemental material). The putative *BcATG8* homologue (Bcin02g02570) was retrieved by BLASTP searches against the *B. cinerea* genome database (http://fungi.ensembl.org/Botrytis_cinerea/Info/Index) using the *S. cerevisiae* Atg8 protein as a query. *BcATG8*, a 669-bp gene with 2 introns, is predicted to encode a 123-amino-acid protein that shares 78% identity with *S. cerevisiae* Atg8.

To characterize *BcATG8*, we first tested whether this gene is able to complement the defects of the yeast counterpart. Yeast expression vector pYES2 containing the full-length cDNA of *BcATG8* was transformed into the yeast *ATG8* null (Δ*Atg8*) mutant (YBL078C). The wild-type (WT) strain BY4741 and the Δ*Atg8* mutant transformed with the empty pYES2 vector served as the positive and negative control, respectively. As shown by the results in Fig. 1A, the tolerance of the Δ*Atg8* mutant for nitrogen starvation was restored by genetic complementation of the mutant with *BcATG8*, indicating that *BcATG8* and *ATG8* share a conserved function associated with autophagy.

A direct protein-protein interaction between Atg8 and Atg4 has been described in *S. cerevisiae* (23). To show that BcAtg8 and BcAtg4 interact with each other in *B. cinerea*, yeast two-hybrid analysis was performed. As shown by the results in Fig. 1B, the yeast

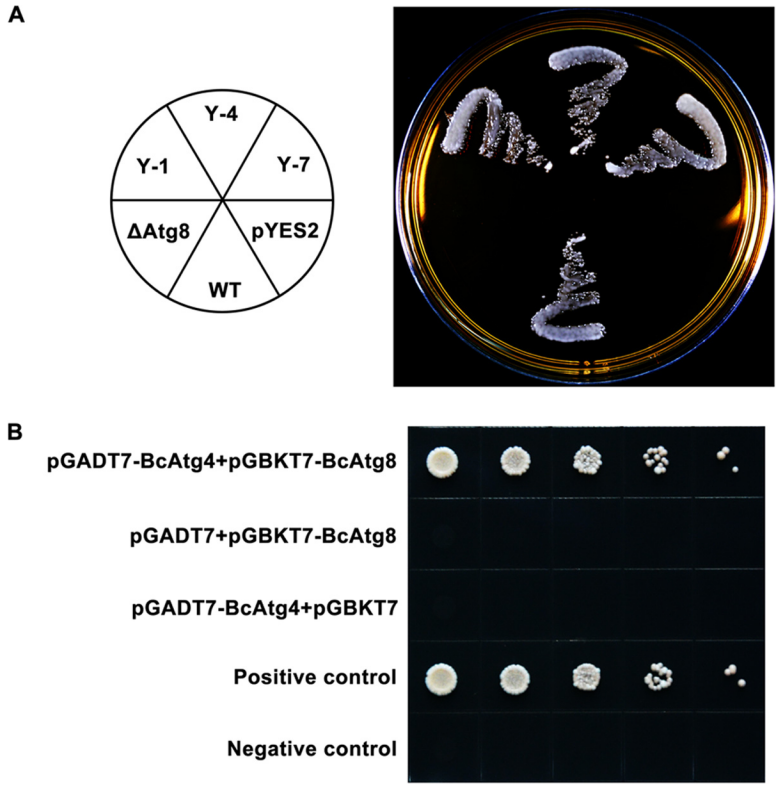

FIG 1 Evolutionary analysis of *BcATG8*. (A) Complementation of yeast *ATG8* null mutant with *BcATG8*. In contrast to the wild-type (WT) yeast, the *ATG8* mutant (Δ*Atg8*) and the mutant transformed with the empty pYES2 vector (pYES2) died after nitrogen starvation, while the mutants transformed with pYES2-BcATG8 (Y-1, Y-4, and Y-7) survived similarly to the WT. (B) Yeast two-hybrid analyses for interaction between BcAtg8 and BcAtg4. Serial dilutions of yeast cells transformed with bait and prey constructs indicated in the figure were examined on SD-Leu-Trp-His plates. The plasmid pair pGADT7 and pGBKT7-53 served as a positive control, and pGADT7 and pGBKT7-Lam served as a negative control.

two-hybrid experiment clearly demonstrated an interaction between BcAtg8 and BcAtg4.

Subcellular localization of GFP-BcAtg8. To visualize autophagy in *B. cinerea*, the green fluorescent protein (GFP)-BcAtg8 fusion construct (BcAtg8 N-terminal fusion with GFP), which is driven by the constitutive *oliC* promoter from *Aspergillus nidulans*, was introduced into the *BcATG8* deletion mutants. Compared with the results for the Δ*BcAtg8* mutant, the mutants expressing GFP-BcAtg8 recovered from the defects in growth and development (data not shown), which indicated that GFP-BcAtg8 is functional. Fluorescence microscopy revealed that GFP-BcAtg8 localized in the cytoplasm as punctate structures in conidia (Fig. 2A), while during conidial germination, it was diffused in the cytoplasm and concentrated in the nuclei of germlings (Fig. 2B). When mycelia were cultured in nitrogen-rich medium (complete medium [CM]), GFP-BcAtg8 localized in the cytoplasm as preautophagosomal structures (PAS), but it mainly accumulated in the lumen of vacuoles under conditions of nitrogen starvation or rapamycin induction (Fig. 3A).

Analysis of autophagy process using GFP-BcAtg8 marker. GFP-Atg8 is now widely used to monitor autophagy, and the process of autophagic flux can be observed by monitoring the vacuolar delivery and subsequent breakdown of GFP-Atg8 (24). In this study, GFP-BcAtg8 appeared as punctate structures that were proximal to the vacuole in the WT under nutrient-rich conditions, but few fluorescent dots were observed in the Δ*BcAtg1* mutant (Fig. 3A). After 6 h of nitrogen starvation or rapamycin induction, the lumen of the vacuoles became obviously fluorescent in the WT; however, no green fluorescence was observed in the vacuoles of the Δ*BcAtg1* mutant (Fig. 3A),

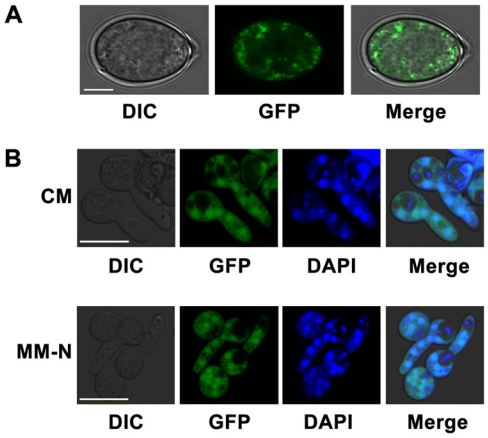

FIG 2 Subcellular localization of GFP-BcAtg8. The GFP-BcAtg8 fused construct was introduced into the wild-type strain to examine the localization of BcAtg8 in fungal cells in various developmental stages. (A) GFP-BcAtg8 presented as punctate structures in conidia. (B) GFP-BcAtg8 was diffused in the cytoplasm and concentrated in the nuclei of germlings. The nuclei were stained by DAPI (4′,6-diamidino-2-phenylindole) and examined by fluorescence microscopy. DIC, differential interference contrast; CM, complete medium; MM-N, minimal medium without $(NH_4)_2SO_4$. Scale bars, 10 μm.

in which autophagy has been verified to be blocked (25). The strain transformed with only the GFP gene showed an evenly diffused GFP signal in the cytoplasm of mycelia.

For a more systematic evaluation, GFP-Atg8 proteolysis assays were performed. Under nutrient-rich conditions, a clear, full-length GFP-BcAtg8 band (40 kDa) was

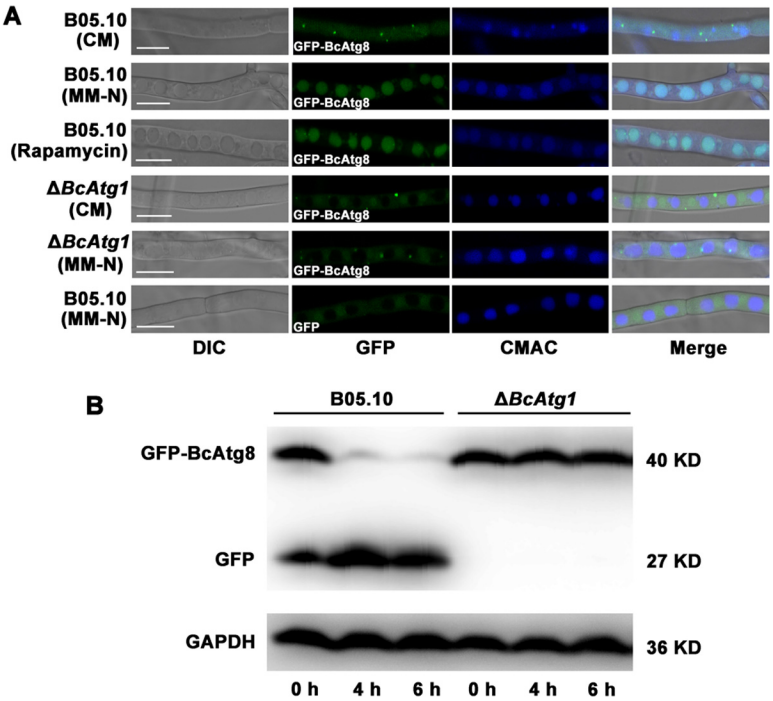

FIG 3 Analysis of autophagy process using GFP-BcAtg8 marker in *B. cinerea*. (A) GFP-BcAtg8 localized in the cytoplasm as preautophagosomal structures (PAS) under nutrient-rich conditions; with induction by starvation or rapamycin, the autophagy process was activated and GFP-BcAtg8 transferred to vacuoles. The vacuoles were stained with CMAC (7-amino-4-chloromethylcoumarin) and examined by fluorescence microscopy. DIC, differential interference contrast; CM, complete medium; MM-N, minimal medium without $(NH_4)_2SO_4$. Scale bars, 10 μm. (B) GFP-BcAtg8 proteolysis assays of B05.10 and the Δ*BcAtg1* mutant. Mycelia were cultured at 25°C for 48 h in CM liquid medium, and autophagy was induced after 4 or 6 h of nitrogen starvation. Mycelia were collected at the indicated times, and mycelial extracts were analyzed by anti-GFP antibody Western blotting. GAPDH was used as an internal reference.

TABLE 1 Oligonucleotide primers used in this study

Primer	Sequence (5′–3′)[a]	Purpose
YC-BcATG8-F	TCACACTGGCGGCCGCTCGAGATGCGATCCAAGTTTAAGGACG	Amplification of full cDNA sequence of the *BcATG8* gene for yeast complementation assays
YC-BcATG8-R	CCCTCTAGATGCATGCTCGAGTTAGTTGGCTTCTTCTAAAGCTTCAC	
Y2H-BcAtg4-F	GCCATGGAGGCCAGTGAATTCATGACGGCGGCTGATTTAGG	Amplification of full cDNA sequence of the *BcATG4* gene for yeast two-hybrid assays
Y2H-BcAtg4-R	ATGCCCACCCGGGTGGAATTCTTAGGCGTCTAATATGGTATCGTCA	
Y2H-BcAtg8-F	ATGGCCATGGAGGCCGAATTCATGCGATCCAAGTTTAAGGACG	Amplification of full cDNA sequence of the *BcATG8* gene for yeast two-hybrid assays
Y2H-BcAtg8-R	TCGACGGATCCCCGGGAATTCTTAGTTGGCTTCTTCTAAAGCTTCAC	
P1	GGTGGTAGCAGGACAAGAC	Amplification of *BcATG8* upstream fragment for construction of the gene deletion vector
P2	CAAAATAGGCATTGATGTGTTGACCTCCTGTAATGGAGGATGATGGAG	
P3	CTCGTCCGAGGGCAAAGGAATAGAGTAGCGCTTCCTTAGACACTTCAG	Amplification of *BcATG8* downstream fragment for construction of the gene deletion vector
P4	ACCATCCTCTTCACTTCTAC	
P5	TATACCTACCTGTCTAGAGAC	Amplification of the *BcATG8* gene deletion vector
P6	AGCTACTCAAGTCATGATTC	
P7	TCAGCATCAGAATAAGCATC	Identification of *BcATG8* deletion transformants
P8	TCCAAAGAGCATACACAACT	
HPH-F	GGAGGTCAACACATCAATGCCTATT	
HPH-R	CTACTCTATTCCTTTGCCCT	Amplification of the hygromycin resistance gene, *HPH*
BcATG8-C-F	ccggaattccggGAGCGAGAGCGAGAGAAGTC	Amplification of full-length *BcATG8*, including 1,116-bp upstream and 92-bp downstream fragments, for complementation of the *BcATG8* deletion mutant
BcATG8-C-R	cgcggatccgcgGTAATGTAGTCACACTGCCC	
GFP-BcAtg8-F	CTTGGGAATGGATGAACTTTACAAAATGCGATCCAAGTTTAAGGACG	Amplification of full-length *BcATG8* fragment used for construction of the GFP-BcAtg8 vector
GFP-BcAtg8-R	TAATCATACATCTTATCTACATACGTTAGTTGGCTTCTTCTAAAGC	
YG8-F	CTCGTGCCGAGGTTAAGTTC	Identification of the in-frame GFP-BcAtg8 fusion vector
YG8-R	CATCCTCATCCTTATGCTCC	
Probe-F	GGTGGTAGCAGGACAAGACT	Amplification of *BcATG8* upstream fragment used as the probe for Southern blot analysis
Probe-R	TGTAATGGAGGATGATGGAG	
A-F	AGCGGAGCAATCGATGTTATAG	Amplification of the BC1G_13009 gene in quantitative real-time PCR assays
A-R	TATGGCCGAAGGAGAGAGAA	
B-F	GGCTTGCGTCTGTGTCTAA	Amplification of the BC1G_11851 gene in quantitative real-time PCR assays
B-R	CGCCTCCAACAACGATAGTAA	
C-F	CCTCCGTTCAATCGATGTTCT	Amplification of the BC1G_10262 gene in quantitative real-time PCR assays
C-R	GCGAGACTCTTGAGGTGTATTC	
D-F	GGGTGAGCAGATCAAGGATATT	Amplification of the BC1G_07580 gene in quantitative real-time PCR assays
D-R	GTCAGATGTGGGTGGGATTT	
E-F	GGAAAGGGAGGAGTACCAAATC	Amplification of the BC1G_03357 gene in quantitative real-time PCR assays
E-R	GGGTTACAGAAGACCCGTAAAG	
F-F	CTTCATCCCTCTACCTCGAAATC	Amplification of the BC1G_12236 gene in quantitative real-time PCR assays
F-R	CCCTTTCACAACCGCATCTA	
G-F	CAGCGTACCCTCATCTGTATTC	Amplification of the BC1G_09602 gene in quantitative real-time PCR assays
G-R	GGGCTCGTCATCGTACATTT	
H-F	CCCGTCGTCATTCACAAGAA	Amplification of the BC1G_07986 gene in quantitative real-time PCR assays
H-R	TAACTCCCGCTCCCATCATA	
Actin-F	CGTCACTACCTTCAACTCCATC	Amplification of the actin gene in quantitative real-time PCR assays
Actin-R	CGGAGATACCTGGGTACATAGT	

[a]Restriction enzyme sites included in primers are in lowercase.

detected in anti-GFP antibody Western blot analysis of the WT, and when mycelia were shifted to nitrogen starvation conditions, the levels of free GFP increased with time, apparently at the expense of full-length GFP-BcAtg8 (Fig. 3B). In the Δ*BcAtg1* mutant, the full-length GFP-BcAtg8 band stayed intact even under nitrogen starvation conditions, suggesting that GFP-BcAtg8 proteolysis was completely interrupted (Fig. 3B). These results indicate that GFP-BcAtg8 is a useable marker to monitor the autophagy process in *B. cinerea*.

Construction of *BcATG8* deletion and complemented mutants. To investigate the role of *BcATG8* in *B. cinerea*, we generated gene deletion mutants using a homologous recombination strategy (Fig. S1A). Four putative deletion mutants were identified from 36 hygromycin-resistant transformants by PCR analysis with primer pair P7/P8 (Table 1). The Southern blot hybridization pattern further confirmed that the Δ*BcAtg8* gene deletion mutant resulted from anticipated homologous recombination events at the *BcATG8* locus and the complemented Δ*BcAtg8-C* strain contains a single copy of the WT *BcATG8*, which was inserted ectopically into the genome of the Δ*BcAtg8* mutant (Fig. S1B).

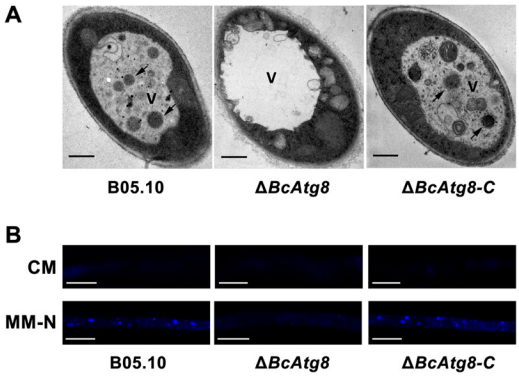

FIG 4 *BcATG8* is required for autophagy. (A) Transmission electron microscopy observation of mycelia of the wild-type strain B05.10, the *BcATG8* deletion mutant (Δ*BcAtg8*), and the complemented strain Δ*BcAtg8-C* cultured in nitrogen-limiting medium (MM-N) with 2 mM PMSF for 6 h. Arrows indicate autophagic bodies. V, vacuole. Scale bar, 0.5 μm. (B) The starved mycelia of each strain were stained with the fluorescent dye MDC (monodansylcadaverine) and observed under a fluorescence microscope. There was no fluorescence observed for all strains grown in CM (complete medium) or for the Δ*BcAtg8* strain grown in MM-N. Scale bar, 10 μm.

The autophagy process is blocked in the Δ*BcAtg8* strain. Using transmission electron microscopy (TEM), we tested the ability of the Δ*BcAtg8* strain to undergo autophagy in response to nitrogen starvation. After mycelia were starved in the presence of phenylmethylsulfonyl fluoride (PMSF) for 6 h, autophagic bodies accumulated in the vacuoles of the WT and complemented strains, while the vacuoles of the Δ*BcAtg8* strain showed normal morphology without any autophagic bodies (Fig. 4A).

Moreover, the autophagy process was analyzed by monodansylcadaverine (MDC) staining, which is an indicator of autophagic activity (26). As shown by the results in Fig. 4B, faint fluorescence was observed in each strain under nitrogen-rich conditions; however, the WT and complemented strains displayed strong fluorescence in the cytoplasm and vacuoles under nitrogen starvation conditions, and only weak fluorescence was observed in the starved mycelia of the Δ*BcAtg8* strain. Therefore, *BcATG8* is essential for autophagy in *B. cinerea*.

***BcATG8* is involved in vegetative growth.** Autophagy plays a role in nutrient trafficking, and *ATG8* is known to be important for vegetative growth (9). Thus, we tested the mycelial growth of the Δ*BcAtg8* mutant under different nutrient conditions. After each strain was cultured on solid medium at 25°C for 4 days, the Δ*BcAtg8* mutant showed significantly reduced growth rates on PDA (potato dextrose agar), MM (minimal medium), and MM-N (minimal medium lacking a nitrogen source) plates compared with the growth rates of the WT and complemented strains (Fig. 5A and B), while there was no significant difference in growth rates on CM plates. In addition, the Δ*BcAtg8* mutant exhibited a distinct colony morphology with fewer aerial hyphae (Fig. 5A). These results suggest that *BcATG8* plays an important role in vegetative growth.

***BcATG8* is required for conidiation, conidial germination, and sclerotial formation.** To test the conidiation of the Δ*BcAtg8* mutant, each strain was incubated on PDA plates at 25°C with a 12-h photophase, but the Δ*BcAtg8* strain failed to produce conidia after 10 days. As *B. cinerea* produces conidia easily on potato, the conidiation was also examined on sterilized potato fragments. When each strain was incubated on autoclaved potato fragments for 10 days, both the WT and complemented strains produced extensive aerial hyphae covered with a dense layer of conidia, while the Δ*BcAtg8* strain failed to form a conidial layer (Fig. 6A). The amount of conidia of the Δ*BcAtg8* mutant was reduced to approximately 60% of that of the WT strain (Fig. 6B).

To examine the role of *BcATG8* in conidial germination, conidia of each strain were cultured in CM (complete medium) and MM-N (lacking nitrogen source) on a hydrophobic surface at 25°C for germination. Although both the WT and Δ*BcAtg8* strains presented similar germination rates in CM at 20 h after inoculation, the germination

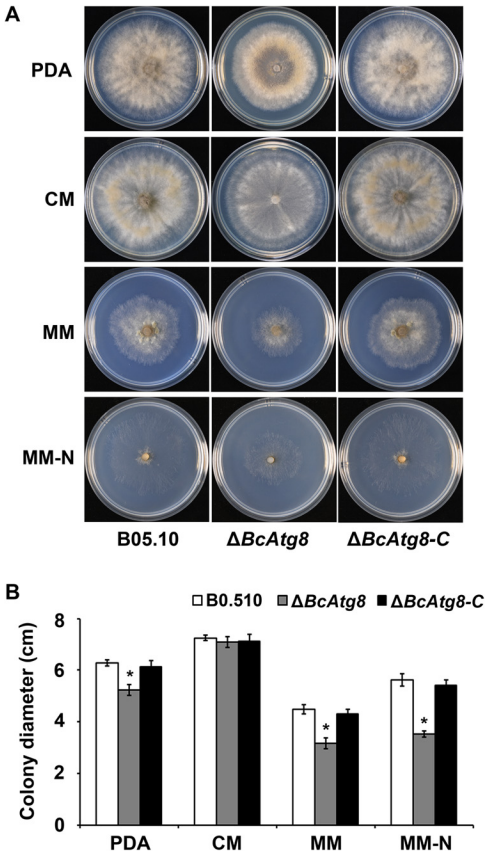

FIG 5 Impacts of *BcATG8* deletion on mycelial growth. (A) Colonies of the wild-type strain B05.10, the *BcATG8* deletion mutant (Δ*BcAtg8*), and the complemented strain Δ*BcAtg8-C* after growth on various media at 25°C for 4 days. PDA, potato dextrose agar; CM, complete medium; MM, minimal medium; MM-N, MM without $(NH_4)_2SO_4$. (B) Statistical analysis of the colony diameters of the indicated strains. Error bars denote standard errors of the results from three repeated experiments, and asterisks indicate statistically significant differences ($P < 0.01$).

rate of the Δ*BcAtg8* strain conidia on MM-N was significantly decreased (Fig. 6C). These results indicated that *BcATG8* is likely to regulate nitrogen source utilization during conidial germination.

Sclerotial formation within dying host tissues in a freezing environment is vital for *B. cinerea* to complete the whole life cycle (3). We therefore investigated the effect of *BcATG8* on sclerotial formation. When mycelia permeated PDA plates at 25°C, they were placed in a 4°C incubator, and after 4 weeks of incubation in the dark, sclerotia were observed only on the WT and the complemented strains (Fig. 6D). These results indicate that *BcATG8* is crucial for reproductive development in *B. cinerea*.

***BcATG8* is required for plant infection.** To investigate the involvement of *BcATG8* in virulence, infection tests on different host tissues were performed. The Δ*BcAtg8* strain failed to infect wounded leaves of cucumber and tomato plants after inoculation for 60 h, while the WT and the complemented strains caused serious disease lesions (Fig. 7A and B). Interestingly, the Δ*BcAtg8* strain showed slight virulence on wounded apple and grape fruits. After incubation for 72 h, the Δ*BcAtg8* strain caused very small disease lesions, whereas the disease lesions caused by the WT and complemented strains were very obvious (Fig. 7C to E). The results suggest that *BcATG8* is essential for full virulence of *B. cinerea*.

***BcATG8* is involved in LD metabolism.** It has been reported that autophagy regulates lipid metabolism in eukaryotic cells (27). To assess the effect of *BcATG8* on lipid droplets (LDs), conidia of each strain were stained with Nile red, a selective fluorescent stain for intracellular lipid droplets (28), and observed by fluorescence

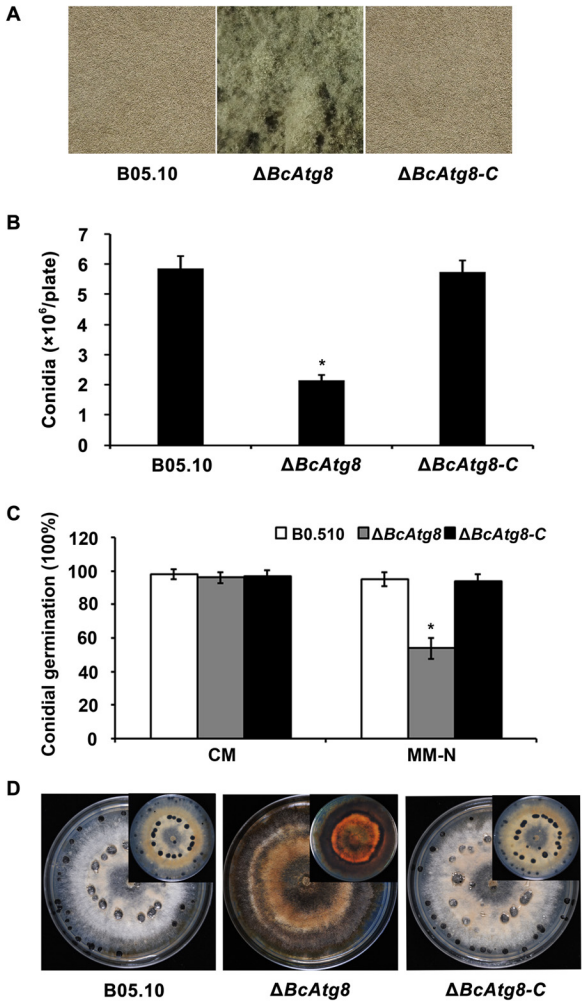

FIG 6 Involvement of *BcATG8* in modulating conidiation, germination, and sclerotial formation. (A) The morphology of conidiation among the wild-type strain B05.10, the *BcATG8* deletion mutant (Δ*BcAtg8*), and the complemented strain Δ*BcAtg8-C* grown on sterilized potato fragments at 25°C with a 12-h photophase for 10 days. (B) The conidia produced by B05.10, the Δ*BcAtg8* strain, and Δ*BcAtg8-C* were washed from each fragment and counted under the microscope. (C) Conidial germination rates of B05.10, the Δ*BcAtg8* strain, and Δ*BcAtg8-C* on a hydrophobic surface in CM or MM-N after 20 h of incubation at 25°C. CM, complete medium; MM-N, minimal medium without $(NH_4)_2SO_4$. Error bars denote standard errors of the results from three repeated experiments, and asterisks indicate statistically significant differences ($P < 0.01$); the error bars and asterisks apply to both panels B and C. (D) Comparison of sclerotial formation among B05.10, the Δ*BcAtg8* strain, and Δ*BcAtg8-C* after 4 weeks of incubation on PDA at 4°C in the dark. PDA, potato dextrose agar. The top-right inset view in each panel is the back of the petri dish.

microscopy. As shown by the results in Fig. 8A, the conidia of the Δ*BcAtg8* strain contained less abundant lipid bodies than those of the WT or of the complemented strain.

To further investigate the impaired LD accumulation in the Δ*BcAtg8* strain, we analyzed the expression of LD metabolism-related genes (Table S1) with quantitative real-time PCR (qRT-PCR). Almost all of the LD degradation and biosynthesis-related genes in the Δ*BcAtg8* strain showed low expression levels compared with their expression in the WT strain (Fig. 8B). Interestingly, the expression of the LD biosynthesis-related gene BC1G_11851, which encodes a diacylglycerol acyltransferase, was significantly higher than in the WT strain (Fig. 8B). These results indicate that the disrupted LD homeostasis in the Δ*BcAtg8* strain is concomitantly associated with LD metabolism.

DISCUSSION

The most basic function of autophagy is to recycle cytoplasmic components that serve as an adaptive mechanism for nutrient starvation (29). The current understanding

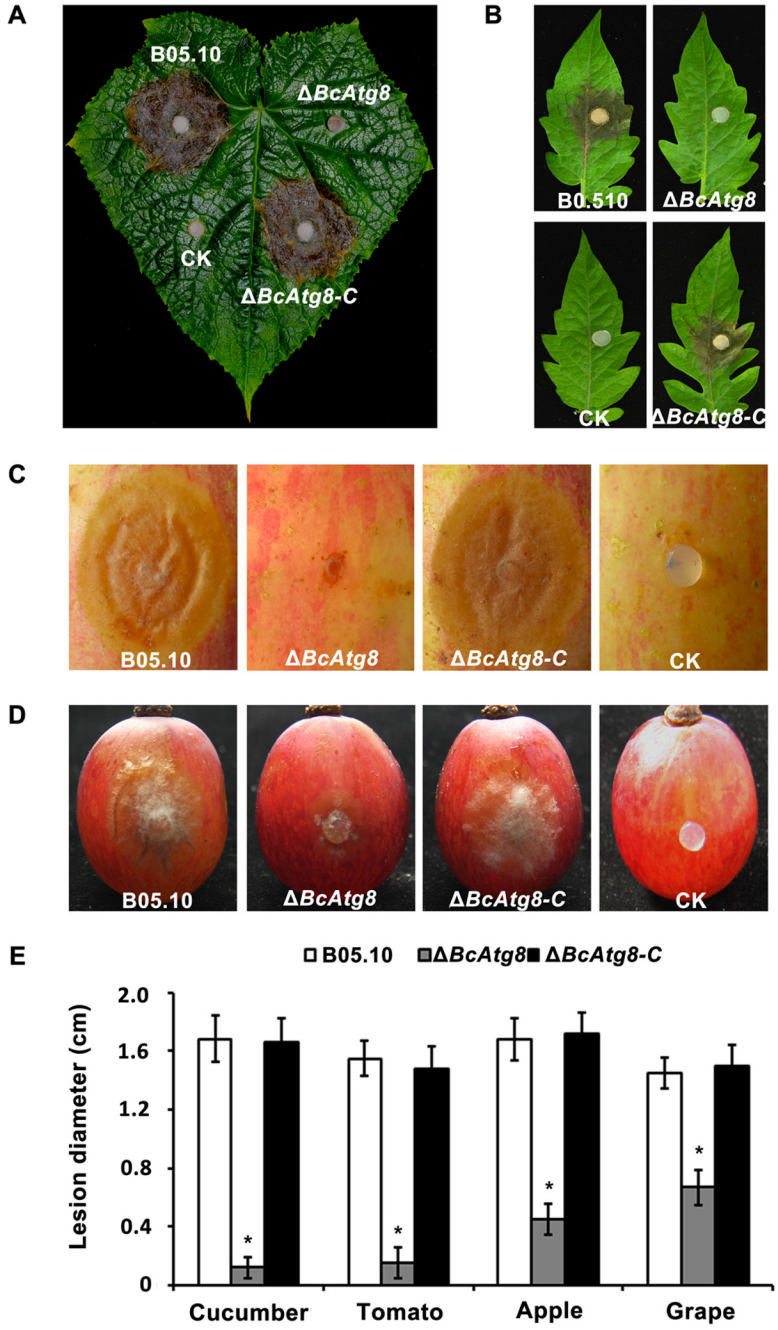

FIG 7 Infection tests on different host plant tissues. The plant tissue samples were incubated with the wild-type strain B05.10, the *BcATG8* deletion mutant (Δ*BcAtg8*), and the complemented strain Δ*BcAtg8-C*. Agar plugs without fungal mycelia were used as negative controls (CK). (A to D) Disease symptoms on wounded cucumber leaves 60 h postinoculation (h.p.i.) (A), wounded tomato leaves 60 h.p.i. (B), wounded apple fruits 72 h.p.i. (C), and wounded grape fruits 72 h.p.i (D). (E) Diameters of disease lesions caused by each strain on different plant tissues. Error bars denote standard errors of the results from five repeated experiments, and asterisks indicate statistically significant differences ($P < 0.01$).

has described autophagy as an integral part of the cellular machinery that facilitates the programmed cell-developmental changes that occur during organ or tissue remodeling in organisms (30, 31). Autophagy has been studied in some kinds of filamentous fungi, especially the plant pathogen *M. oryzae* (8). Deletion of various autophagy-related genes has revealed that autophagy is required for vegetative growth, asexual and sexual development, life span, secondary metabolism, and pathogenicity (18, 21, 22,

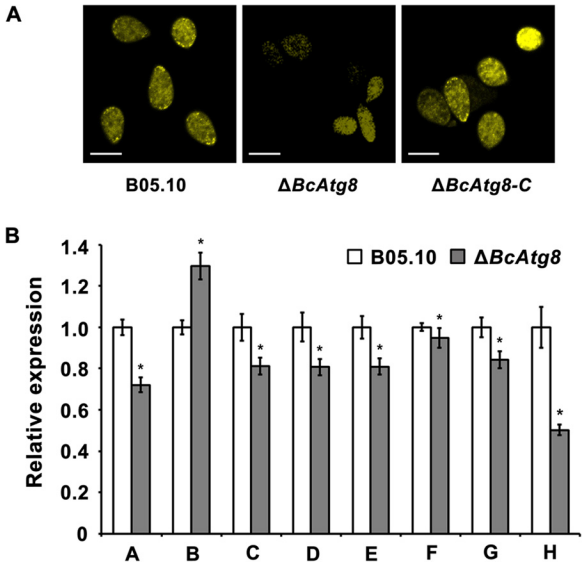

FIG 8 Involvement of *BcATG8* in the regulation of lipid metabolism. (A) Lipid droplets in conidia were stained with Nile red and examined under a microscope with episcopic fluorescence. Scale bars, 20 μm. (B) Relative transcription levels of lipid droplet biosynthesis-related genes in the wild-type strain B05.10 and the *BcATG8* deletion mutant (Δ*BcAtg8*). Genes tested are as follows. Lipid droplet biosynthesis-related genes: A, BC1G_13009; B, BC1G_11851; and C, BC1G_10262. Degradation-related genes: D, BC1G_07580; E, BC1G_03357; F, BC1G_12236; G, BC1G_09602; and H, BC1G_07986. Error bars denote standard errors from three repeated experiments, and asterisks indicate statistically significant differences ($P < 0.01$).

32–34). The previous study we made in *B. cinerea* suggests that *BcATG1* is involved in fungal development and pathogenesis (25). To further understand autophagy in *B. cinerea*, we isolated *BcATG8*, a yeast *ATG8* homologue in *B. cinerea*, visualized the autophagy process using a fluorescent fusion protein, and further analyzed its function by a reverse genetic approach.

In yeast, Atg8 is posttranslationally modified at its C terminus by the cysteine protease Atg4 to expose Gly116, thus allowing Atg8 to conjugate with phosphatidylethanolamine (PE) in a ubiquitin-like reaction catalyzed by Atg7 and Atg3 that results in targeting to autophagosomal membranes (13, 23). In *B. cinerea*, BcAtg8 has a conserved Gly residue at the C terminus as well, which together with the results of the yeast complementation and yeast-two hybrid assays (Fig. 1), suggests the evolutionary conservation of this conjugation system.

The occurrence of autophagy can be directly visualized by fluorescent-marker-tagged Atg8, which localizes to autophagosome(s) and is internalized in vacuole(s) after fusion between autophagosomes and vacuoles (35). Here, we constructed complemented strains expressing GFP-BcAtg8, whose expression was driven by a constitutive promoter in the *BcATG8* mutants. In these strains, the phenotypic defects of *BcATG8* mutants were totally complemented, suggesting that the GFP-BcAtg8 fusion protein is competent as a replacement for the native BcAtg8 protein. The subcellular localization of the GFP signals observed in conidia, germlings, and mycelia indicated that nitrogen starvation and rapamycin are stimuli for autophagy (Fig. 2 and 3).

Fluorescence microscopy showed that GFP-BcAtg8 was localized in vacuoles when autophagy was induced, while deletion of *BcATG1* blocked GFP-BcAtg8 from transferring from cytoplasm to vacuoles under starvation conditions (Fig. 3A). In addition, the GFP-BcAtg8 proteolysis assays further confirmed that autophagy was blocked in the *BcATG8* mutant (Fig. 3B). Therefore, a similar system of autophagy takes place in *B. cinerea*.

To elucidate the functions of *BcATG8* in *B. cinerea*, targeted gene deletion mutants were constructed. Similar to what has been reported for other filamentous fungi, loss of *ATG8* leads to blocking of the autophagy process after starvation or treatment with

rapamycin in *B. cinerea*, thus limiting autophagy (Fig. 4). In addition, the general phenotypes, including defects in growth, conidiation, sclerotium formation, and pathogenicity, were also seen for *BcATG8* mutants.

During growth under adverse conditions, endogenous recycling of the cytosol and organelles by autophagy is believed to be important for nutrient trafficking along hyphal filaments, as well as for the development of aerial hyphae bearing conidiophores (36). In line with this idea, *BcATG8* mutants exhibited reduced aerial hyphae (Fig. 5) and conidiation (Fig. 6A and B), as reported in other filamentous fungi (15, 18, 21, 22, 37). In the initial stage of conidiation, autophagic degradation may produce abundant nutrients and small molecules for energy sources or materials to build up new intracellular structures. Additionally, the *BcATG8* mutants completely lost the ability to form sclerotium (Fig. 6D), which is consistent with the results for *AoATG1* and *AoATG8* mutants of *A. oryzae* (38). These findings imply that the involvement of autophagy in asexual reproduction is conserved in filamentous fungi.

In *A. oryzae*, the *AoATG8* mutants exhibited a slight delay in conidial germination in the absence of nitrogen sources (18). In *B. cinerea*, GFP-BcAtg8 was diffused in the cytoplasm and concentrated in the nuclei of germlings (Fig. 2B), which suggests that the autophagy process is activated during conidial germination. Here, the *BcATG8* mutants showed nearly the same conidial germination rate as the WT strain in complete medium (CM), while germination in medium lacking nitrogen sources (MM-N) was delayed (Fig. 6C), indicating that autophagy was at least partly involved in supplying a nitrogen source at an early stage of conidial germination.

In fungal pathogens, successful infection might depend on the recycling of macromolecules to support cellular activity under adverse conditions in the host, which is particularly important because nutrient deprivation may commonly occur during such growth phases of development and morphogenesis (39). Similar to findings for other plant-pathogenic fungi (8), which require autophagy for infection, deletion of *BcATG8* in *B. cinerea* also led to significantly attenuated pathogenicity on various host plants (Fig. 7). Thus, autophagy is a prerequisite for infection and perhaps constitutes a further developmental checkpoint for growth in plant tissue.

Eukaryotic cells store excess fatty acids as neutral lipids, predominantly triacylglycerols and sterol esters, in organelles termed lipid droplets (LDs). The contents of LDs, predominantly triacylglycerols (TAGs) and sterol esters (SEs), provide cells with membrane and energy sources and also protect cells against lipotoxicity (40). Recent research has shown that LDs serve as a substrate for autophagy, and the ability to undergo autophagy in response to changes in nutrient supply allows the cell to alter LD metabolism to meet cellular energy demands (41). In *M. oryzae*, the accumulated content of LDs in conidia is affected by autophagy, and lipid droplets in conidia are much less abundant in the *MoATG8* mutant (19). In this study, deletion of *BcATG8* dramatically reduced the amount of LDs in conidia (Fig. 8A), which was also consistent with the results in the *ATG8* mutants of *M. robertsii* (22). Furthermore, the differential expression of the LD metabolism-associated genes between the WT strain and *BcATG8* mutants (Fig. 8B) implies that the impact of autophagy on LD storage is partly influenced by the imbalance of lipid metabolism.

In conclusion, our study demonstrates that the autophagy gene *BcATG8* plays a pleiotropic role in *B. cinerea*, including mycelial growth, reproductive development, lipid metabolism, and plant infection. Further study would certainly aim at the specific mechanisms of autophagy in cell differentiation and development in *B. cinerea*.

MATERIALS AND METHODS

Fungal strains and culture conditions. *Botrytis cinerea* strain B05.10 was used as the parental strain for transformation experiments and as the WT control. *B. cinerea* strains were grown on potato dextrose agar (PDA; 200 g potato, 20 g dextrose, 20 g agar, and 1 liter water), complete medium (CM; 1% glucose, 0.2% peptone, 0.1% yeast extract, 0.1% Casamino Acids, nitrate salts [6 g $NaNO_3$, 0.52 g KCl, 0.52 g $MgSO_4 \cdot 7H_2O$, 1.52 g KH_2PO_4], trace elements, 0.01% vitamins [biotin, pyridoxine, thiamine, riboflavin, *p*-aminobenzoic acid, and nicotinic acid], and 1 liter water, pH 6.5), and minimal medium [MM; 10 mM K_2HPO_4, 10 mM KH_2PO_4, 4 mM $(NH_4)_2SO_4$, 2.5 mM NaCl, 2 mM $MgSO_4$, 0.45 mM $CaCl_2$, 9 mM $FeSO_4$, 10 mM glucose, and 1 liter water, pH 6.9] at 25°C for mycelial growth. Sterilized potato fragments were used

for conidiation assays. PDA was used for sclerotial formation assays. MM-N [MM without $(NH_4)_2SO_4$] was used for autophagy induction. Yeast WT strain BY4741 and the *ATG8* null mutant (Δ*Atg8*) (YBL078C) were cultured in YPD (1% yeast extract, 2% peptone, and 2% glucose) and synthetic defined medium lacking a nitrogen source (SD-N; 2% glucose and 0.17% yeast nitrogen base without amino acids and ammonium sulfate) at 30°C.

Sequence analysis of *BcATG8*. The *ATG8* homologue in *B. cinerea* was originally identified through homology searches of the *B. cinerea* genome database (http://www.broadinstitute.org/annotation/genome/botrytis_cinerea/) by using the BLASTP algorithm with *ATG8* from *S. cerevisiae* as the query. To verify the existence and size of introns in *BcATG8*, total RNA was extracted from mycelia of the WT strain B05.10 with an RNAsimple total RNA kit (Tiangen Biotech Co., Ltd., Beijing, China) and used for reverse transcription with a HiScript II 1st-strand cDNA synthesis kit (Vazyme Biotech Co., Ltd., Nanjing, China). The coding region of *BcATG8* was amplified using the cDNA as the template and primer pair YC-BcATG8-F and YC-BcATG8-R (Table 1). The resulting PCR product was purified, cloned, and sequenced.

Yeast complementation. The full-length cDNA of *BcATG8* was cloned into the yeast expression vector pYES2 (Invitrogen, Carlsbad, CA) and transformed into the yeast *ATG8* null mutant using the lithium acetate (LiAc)/single-stranded DNA (ssDNA)/polyethylene glycol (PEG) transformation protocol (42). Yeast transformants were selected on SD medium lacking uracil (Clontech, Palo Alta, CA). In addition, the WT strain BY4741 and the Δ*Atg8* mutant transformed with the empty pYES2 vector were used as positive and negative controls, respectively. For complementation assays, the yeast transformants were cultured on YPD medium for 2 days at 30°C and then moved to SD-N medium for 18 days. The experiment was repeated three times independently.

Yeast two-hybrid assay. To construct plasmids for yeast two-hybrid analyses, the coding region of each tested gene was amplified from the genomic cDNA of B05.10 with the primer pairs listed in Table 1. The cDNA fragments of *BcATG8* and *BcATG4* were inserted into the yeast GAL4 binding domain vector pGBKT7 and GAL4 activation domain vector pGADT7 (Clontech, Mountain View, CA, USA), respectively. The pairs of yeast two-hybrid plasmids were cotransformed into the yeast strain AH109 following the LiAc/SS-DNA/PEG transformation protocol (42). In addition, plasmid pair pGBKT7-53 and pGADT7 served as a positive control, and plasmid pair pGBKT7-Lam and pGADT7 served as a negative control. Transformants were grown at 30°C for 3 days on SD lacking Leu and Trp and then transferred to SD stripped of His, Leu, and Trp and containing 5 mM 3-aminotriazole (3-AT) to assess binding activity. Three independent experiments were performed.

Gene deletion and complementation. The gene replacement construct of *BcATG8* was generated using the double-joint PCR approach (43). Briefly, the upstream and downstream flanking regions of *BcATG8* were amplified and fused with the hygromycin phosphotransferase gene (*HPH*) cassette. The resulting PCR product was transformed into the protoplast of the WT progenitor B05.10 according to a previously described method (44). The putative gene deletion mutants with hygromycin resistance were first screened by PCR and further confirmed by Southern blotting. The primers used to generate the deletion mutant are listed in Table 1.

To construct the vector for complementation of the *BcATG8* deletion mutant, the full-length *BcATG8* gene, containing the 1,437-bp promoter region and 129-bp terminator region, was amplified from the genomic DNA of B05.10 with specific primers (Table 1) and subsequently cloned into KpnI/PstI sites of plasmid pNEO (45). Before transformation, the complementary fragment in the plasmid was sequenced to ensure fidelity with the original sequence of *BcATG8*.

GFP fusion vector construction and fluorescence microscopy. The GFP-BcAtg8 fusion construct (BcAtg8 N-terminal fusion with GFP), which is driven by the *oliC* promoter from *A. nidulans*, was generated according to a method described previously (46), with some modifications. Briefly, the GFP vector pNAN-OGG was digested with NotI and assembled with the PCR fragment comprising the open reading frame of *BcATG8* using a one-step cloning kit (Vazyme Biotech Co., Ltd., Nanjing, China). The recombined plasmid yielded was confirmed by sequencing to contain the in-frame fusion region. For protoplast transformation, the sequenced vector was cut with SacII and ApaI to obtain the linearized GFP-BcAtg8 fusion construct. Nourseothricin-resistant transformants were obtained after transformation and screened by PCR and GFP signal. Samples of the validated strains were observed with a confocal laser scanning microscope (Leica TCS SP8, Leica, Germany). The primers used are listed in Table 1.

Nucleic acid manipulations. Genomic DNA was extracted as described by McDonald and Martinez (47). Plasmid DNA was isolated using a plasmid minikit I (Omega Bio-tek Co., Shanghai, China). Southern blotting was performed using an 1,193-bp upstream fragment of *BcATG8* as a probe, which was labeled with digoxigenin (DIG) according to the protocol of the manufacturer using the high prime DNA labeling and detection starter kit I (Roche Diagnostics, Mannheim, Germany). Genomic DNA extracted from *B. cinerea* was digested with EcoRI restriction endonuclease.

RNA extraction and quantitative real-time PCR. Total RNA was extracted from mycelia using an RNAsimple total RNA kit (Tiangen Biotech Co., Ltd., Beijing, China). The reverse transcription of RNA was carried out using HiScript Q RT supermix for qPCR (plus genomic DNA [gDNA] wiper) (Vazyme Biotech Co., Ltd., Nanjing, China). The real-time PCR amplifications were conducted using an ABI 7500 real-time detection system (Applied Biosystems, Foster City, CA, USA) with ChamQ SYBR qPCR master mix (Vazyme Biotech Co., Ltd., Nanjing, China). Gene expression levels were calculated using the cycle threshold ($2^{-\Delta\Delta CT}$) method (48) with the actin gene as the endogenous reference. The experiment was repeated three times independently.

Monitoring the autophagy process. For TEM observations, the conidia of each strain were cultured in CM liquid medium for 24 h at 25°C in a 180-rpm shaker. The young mycelia were harvested, washed thoroughly in distilled water, and transferred to MM-N liquid medium with 2 mM phenylmethylsulfonyl

fluoride (PMSF). After incubation at 25°C for 6 h, the fungal mass was collected, fixed overnight at 4°C in 2.5% glutaraldehyde, and then rinsed three times with 0.1 M phosphate-buffered saline (PBS). Next, the samples were postfixed in 1% osmic acid for 3 h at 25°C, washed three times with PBS as before, dehydrated in graded ethanol solutions, embedded in resin, and stained with 2% uranyl acetate and Reynold's lead solution before sectioning. The ultrathin sections were examined under a JEM-1230 electron microscope (JEOL, Tokyo, Japan).

For monodansylcadaverine (MDC) staining, the nitrogen-starved mycelia of each strain were stained with MDC at a final concentration of 50 μM for 30 min in the dark. After washing with water, samples were observed with epifluorescence microscopy using a 4′,6-diamidino-2-phenylindole (DAPI) filter.

Protein manipulation and Western blotting. For total protein extractions, mycelia of each strain were ground to a fine powder in liquid nitrogen and resuspended in 1 ml of protein extraction buffer (50 mM Tris-HCl, pH 7.5, 100 mM NaCl, 5 mM EDTA, 1% Triton X-100, 2 mM PMSF) and 10 μl of protease inhibitor cocktail (Sangon, Shanghai, China). After homogenization with a vortex shaker, the lysate was centrifuged at 12,000 $\times$ *g* for 10 min at 4°C. The supernatant was mixed with protein loading buffer and boiled for 5 min. Then, each sample was separated by SDS-PAGE gel and transferred to PVDF (polyvinylidene fluoride) membrane. Monoclonal anti-GFP antibody 32146 (Abcam, Cambridge, MA, USA) was used at a 1:5,000 to 1:10,000 dilution for immunoblot analyses. The samples were also detected with monoclonal anti-glyceraldehyde-3-phosphate dehydrogenase (GAPDH) antibody EM1101 (Hangzhou HuaAn Biotechnology Co., Ltd.) as a reference. The experiment was conducted three times independently.

Histochemical analysis of lipid droplets. Lipid droplets (LDs) in conidia were visualized by staining with Nile red. Briefly, conidia of each strain were harvested and stained directly with Nile red solution (20 mg/ml polyvinylpyrrolidone and 2.5 μg/ml Nile red oxazone [Sigma, St. Louis, MO, USA] in 50 mM Tris-maleate buffer [pH 7.5]). Within a few seconds in the dark, LDs were examined under a microscope with an episcopic fluorescence attachment.

Infection tests. The pathogenicity experiments were performed on cucumber and tomato primary leaves and apple and grape fruits. Briefly, the plant tissues used were point inoculated with mycelial plugs of 3-day-old cultures. Before inoculation, the cuticle of hosts was wounded with a sterilized needle tip to facilitate penetration of the fungus into plant tissues. Additionally, water agar plugs without fungal mycelia were used as negative controls (CK). The inoculated samples were placed in high-relative-humidity conditions (~95%) at 25°C with 16 h of daylight. The diameters of disease lesions were recorded after the times indicated in the figures. These experiments were repeated three times, with at least 10 samples each time.

SUPPLEMENTAL MATERIAL

Supplemental material for this article may be found at https://doi.org/10.1128/AEM.02455-17.

SUPPLEMENTAL FILE 1, PDF file, 0.2 MB.

ACKNOWLEDGMENTS

We thank Julia Schumacher (Westfälische Wilhelms-Universität Münster, Germany) for kindly providing the codon-optimized GFP vectors of *Botrytis cinerea*.

This work was supported by the National Natural Science Foundation of China (31672065), Special Fund for Agro-scientific Research in the Public Interest (201503112-07 and 201303023) and Agricultural Science and Technology Innovation Fund Project of Jiangsu province, China [CX (14) 2054].

REFERENCES

1. Dean R, Van Kan JAL, Pretorius ZA, Hammond-Kosack KE, Di Pietro A, Spanu PD, Rudd JJ, Dickman M, Kahmann R, Ellis J, Foster GD. 2012. The top 10 fungal pathogens in molecular plant pathology. Mol Plant Pathol 13:414–430. https://doi.org/10.1111/j.1364-3703.2011.00783.x.
2. Pande S, Galloway J, Gaur PM, Siddique KHM, Tripathi HS, Taylor P, MacLeod MWJ, Basandrai AK, Bakr A, Joshi S, Krishna Kishore G, Isenegger DA, Narayana Rao J, Sharma M. 2006. Botrytis grey mould of chickpea: a review of biology, epidemiology, and disease management. Aust J Agric Res 57:1137–1150. https://doi.org/10.1071/AR06120.
3. Williamson B, Tudzynski B, Tudzynski P, Van Kan JAL. 2007. *Botrytis cinerea*: the cause of grey mould disease. Mol Plant Pathol 8:561–580. https://doi.org/10.1111/j.1364-3703.2007.00417.x.
4. Klionsky DJ, Emr SD. 2000. Autophagy as a regulated pathway of cellular degradation. Science 290:1717–1721. https://doi.org/10.1126/science.290.5497.1717.
5. Deretic V, Levine B. 2009. Autophagy, immunity, and microbial adaptations. Cell Host Microbe 5:527–549. https://doi.org/10.1016/j.chom.2009.05.016.
6. Reggiori F, Klionsky DJ. 2005. Autophagosomes: biogenesis from scratch? Curr Opin Cell Biol 17:415–422. https://doi.org/10.1016/j.ceb.2005.06.007.
7. Mizushima N, Noda T, Yoshimori T, Tanaka Y, Ishii T, George MD, Klionsky DJ, Oshumi M, Ohsumi Y. 1998. A protein conjugation system essential for autophagy. Nature 395:395–398. https://doi.org/10.1038/26506.
8. Pollack JK, Harris SD, Marten MR. 2009. Autophagy in filamentous fungi. Fungal Genet Biol 46:1–8. https://doi.org/10.1016/j.fgb.2008.10.010.
9. Lu JP, Liu XH, Feng XX, Min H, Lin FC. 2009. An autophagy gene, *MgATG5*, is required for cell differentiation and pathogenesis in *Magnaporthe oryzae*. Curr Genet 55:461–473. https://doi.org/10.1007/s00294-009-0259-5.
10. Klionsky DJ, Cregg JM, Dunn WA, Jr, Emr SD, Sakai Y, Sandoval IV, Sibirny A, Subramani S, Thumm M, Veenhuis M. 2003. A unified nomenclature for yeast autophagy-related genes. Dev Cell 5:539–545. https://doi.org/10.1016/S1534-5807(03)00296-X.
11. Kirisako T, Baba M, Ishihara N, Miyazawa K, Ohsumi M, Yoshimori T, Noda T, Oshumi Y. 1999. Formation process of autophagosome is traced with

Apg8/Aut7p in yeast. J Cell Biol 147:435–446. https://doi.org/10.1083/jcb.147.2.435.
12. Suzuki K, Kirisako T, Kamada Y, Mizushima N, Noda T, Ohsumi Y. 2001. The pre-autophagosomal structure organized by concerted functions of APG genes is essential for autophagosome formation. EMBO J 20:5971–5981. https://doi.org/10.1093/emboj/20.21.5971.
13. Ichimura Y, Kirisako T, Takao T, Satomi Y, Shimonishi Y, Ishihara N, Mizushima N, Tanida I, Kominami E, Oshumi M, Noda T, Oshumi Y. 2000. A ubiquitin-like system mediates protein lipidation. Nature 408:488–492. https://doi.org/10.1038/35044114.
14. Yoshimoto K, Hanaoka H, Sato S, Kato T, Tabata S, Noda T, Ohsumi Y. 2004. Processing of ATG8s, ubiquitin-like proteins, and their deconjugation by ATG4s are essential for plant autophagy. Plant Cell 16:2967–2983. https://doi.org/10.1105/tpc.104.025395.
15. Bartoszewska M, Kiel JAKW. 2010. The role of macroautophagy in development of filamentous fungi. Antioxid Redox Signal 14:2271–2287. https://doi.org/10.1089/ars.2010.3528.
16. Khan IA, Lu JP, Liu XH, Rehman A, Lin FC. 2012. Multifunction of autophagy-related genes in filamentous fungi. Microbiol Res 167:339–345. https://doi.org/10.1016/j.micres.2012.01.004.
17. Pinan-Lucarré B, Paoletti M, Dementhon K, Coulary-Salin B, Clavé C. 2003. Autophagy is induced during cell death by incompatibility and is essential for differentiation in the filamentous fungus *Podospora anserina*. Mol Microbiol 47:321–333. https://doi.org/10.1046/j.1365-2958.2003.03208.x.
18. Kikuma T, Ohneda M, Arioka M, Kitamoto K. 2006. Functional analysis of the *ATG8* homologue Aoatg8 and role of autophagy in differentiation and germination in *Aspergillus oryzae*. Eukaryot Cell 5:1328–1336. https://doi.org/10.1128/EC.00024-06.
19. Veneault-Fourrey C, Barooah M, Egan M, Wakley G, Talbot NJ. 2006. Autophagic fungal cell death is necessary for infection by the rice blast fungus. Science 312:580–583. https://doi.org/10.1126/science.1124550.
20. Deng YZ, Ramos-Pamplona M, Naqvi NI. 2009. Autophagy-assisted glycogen catabolism regulates asexual differentiation in *Magnaporthe oryzae*. Autophagy 5:33–43. https://doi.org/10.4161/auto.5.1.7175.
21. Josefsen L, Droce A, Sondergaard TE, Sørensen JL, Bormann J, Schäfer W, Giese H, Olsson S. 2012. Autophagy provides nutrients for nonassimilating fungal structures and is necessary for plant colonization but not for infection in the necrotrophic plant pathogen *Fusarium graminearum*. Autophagy 8:326–337. https://doi.org/10.4161/auto.18705.
22. Duan Z, Chen Y, Huang W, Shang Y, Chen P, Wang C. 2013. Linkage of autophagy to fungal development, lipid storage and virulence in *Metarhizium robertsii*. Autophagy 9:538–549. https://doi.org/10.4161/auto.23575.
23. Kirisako T, Ichimura Y, Okada H, Kabeya Y, Mizushima N, Yoshimori T, Oshumi M, Takao T, Noda T, Oshumi Y. 2000. The reversible modification regulates the membrane-binding state of Apg8/Aut7 essential for autophagy and the cytoplasm to vacuole targeting pathway. J Cell Biol 151:263–275. https://doi.org/10.1083/jcb.151.2.263.
24. Nair U, Jotwani A, Geng J, Gammoh N, Richerson D, Yen WL, Griffith J, Nag S, Wang K, Moss T, Baba M, McNew JA, Jiang XJ, Reggiori F, Melia TJ, Klionsky DJ. 2011. SNARE proteins are required for macroautophagy. Cell 146:290–302. https://doi.org/10.1016/j.cell.2011.06.022.
25. Ren W, Zhang Z, Shao W, Yang Y, Zhou M, Chen C. 2017. The autophagy-related gene *BcATG1* is involved in fungal development and pathogenesis in *Botrytis cinerea*. Mol Plant Pathol 18:238–248. https://doi.org/10.1111/mpp.12396.
26. Biederbick A, Kern HF, Elsässer HP. 1995. Monodansylcadaverine (MDC) is a specific in vivo marker for autophagic vacuoles. Eur J Cell Biol 66:3–14.
27. Singh R, Kaushik S, Wang Y, Xiang Y, Novak I, Komatsu M, Tanaka K, Cuervo AM, Czaja MJ. 2009. Autophagy regulates lipid metabolism. Nature 458:1131–1135. https://doi.org/10.1038/nature07976.
28. Greenspan P, Mayer EP, Fowler SD. 1985. Nile red: a selective fluorescent stain for intracellular lipid droplets. J Cell Biol 100:965–973. https://doi.org/10.1083/jcb.100.3.965.
29. Klionsky DJ. 2007. Autophagy: from phenomenology to molecular understanding in less than a decade. Nat Rev Mol Cell Biol 8:931–937. https://doi.org/10.1038/nrm2245.
30. Mizushima N. 2007. Autophagy: process and function. Gene Dev 21:2861–2873. https://doi.org/10.1101/gad.1599207.
31. Boya P, Reggiori F, Codogno P. 2013. Emerging regulation and functions of autophagy. Nat Cell Biol 15:713–720. https://doi.org/10.1038/ncb2788.
32. Liu XH, Lu JP, Zhang L, Dong B, Min H, Lin FC. 2007. Involvement of a *Magnaporthe grisea* serine/threonine kinase gene, *MgATG1*, in appressorium turgor and pathogenesis. Eukaryot Cell 6:997–1005. https://doi.org/10.1128/EC.00011-07.
33. Voigt O, Pöggeler S. 2013. Autophagy genes Smatg8 and Smatg4 are required for fruiting-body development, vegetative growth and ascospore germination in the filamentous ascomycete *Sordaria macrospora*. Autophagy 9:33–49. https://doi.org/10.4161/auto.22398.
34. Corral-Ramos C, Roca MG, Di Pietro A, Roncero MIG, Ruiz-Roldán C. 2015. Autophagy contributes to regulation of nuclear dynamics during vegetative growth and hyphal fusion in *Fusarium oxysporum*. Autophagy 11:131–144. https://doi.org/10.4161/15548627.2014.994413.
35. Mizushima N. 2004. Methods for monitoring autophagy. Int J Biochem Cell Biol 36:2491–2502. https://doi.org/10.1016/j.biocel.2004.02.005.
36. Shoji JY, Arioka M, Kitamoto K. 2006. Possible involvement of pleiomorphic vacuolar networks in nutrient recycling in filamentous fungi. Autophagy 2:226–227. https://doi.org/10.4161/auto.2695.
37. Nitsche BM, Burggraaf-van Welzen AM, Lamers G, Meyer V, Ram AFJ. 2013. Autophagy promotes survival in aging submerged cultures of the filamentous fungus *Aspergillus niger*. Appl Microbiol Biotechnol 97:8205–8218. https://doi.org/10.1007/s00253-013-4971-1.
38. Yanagisawa S, Kikuma T, Kitamoto K. 2013. Functional analysis of Aoatg1 and detection of the Cvt pathway in *Aspergillus oryzae*. FEMS Microbiol Lett 338:168–176. https://doi.org/10.1111/1574-6968.12047.
39. Liu XH, Gao HM, Xu F, Lu JP, Devenish RJ, Lin FC. 2012. Autophagy vitalizes the pathogenicity of pathogenic fungi. Autophagy 8:1415–1425. https://doi.org/10.4161/auto.21274.
40. Wang CW. 2015. Lipid droplet dynamics in budding yeast. Cell Mol Life Sci 72:2677–2695. https://doi.org/10.1007/s00018-015-1903-5.
41. Dong H, Czaja MJ. 2011. Regulation of lipid droplets by autophagy. Trends Endocrinol Metab 22:234–240. https://doi.org/10.1016/j.tem.2011.02.003.
42. Schiestl RH, Gietz RD. 1989. High efficiency transformation of intact yeast cells using single stranded nucleic acids as a carrier. Curr Genet 16:339–346. https://doi.org/10.1007/BF00340712.
43. Gronover CS, Kasulke D, Tudzynski P, Tudzynski B. 2001. The role of G protein alpha subunits in the infection process of the gray mold fungus *Botrytis cinerea*. Mol Plant Microbe Interact 14:1293–1302. https://doi.org/10.1094/MPMI.2001.14.11.1293.
44. Yu JH, Hamari Z, Han KH, Seo JA, Reyes-Domínguez Y, Scazzocchio C. 2004. Double-joint PCR: a PCR-based molecular tool for gene manipulations in filamentous fungi. Fungal Genet Biol 41:973–981. https://doi.org/10.1016/j.fgb.2004.08.001.
45. Duan Y, Ge C, Liu S, Wang J, Zhou M. 2013. A two-component histidine kinase Shk1 controls stress response, sclerotial formation and fungicide resistance in *Sclerotinia sclerotiorum*. Mol Plant Pathol 14:708–718. https://doi.org/10.1111/mpp.12041.
46. Schumacher J. 2012. Tools for *Botrytis cinerea*: new expression vectors make the gray mold fungus more accessible to cell biology approaches. Fungal Genet Biol 49:483–497. https://doi.org/10.1016/j.fgb.2012.03.005.
47. McDonald BA, Martinez JP. 1990. Restriction fragment length polymorphisms in *Septoria tritici* occur at a high frequency. Curr Genet 17:133–138. https://doi.org/10.1007/BF00312858.
48. Livak KJ, Schmittgen TD. 2001. Analysis of relative gene expression data using real-time quantitative PCR and the $2^{-\Delta\Delta CT}$ method. Methods 25:402–408. https://doi.org/10.1006/meth.2001.1262.